In-depth structural characterization of oligosaccharides released by GH107 endofucanase Mf FcnA reveals enzyme subsite specificity and sulfated fucan substructural features

David Ropartz, Lery Marion, Mathieu Fanuel, Jasna Nikolic, Murielle Jam, Robert Larocque, Elizabeth Ficko-Blean, Gurvan Michel, Hélène Rogniaux

HAL Id: hal-03540768
https://hal.inrae.fr/hal-03540768

Submitted on 28 Oct 2022

In-depth structural characterization of oligosaccharides released by GH107 endofucanase

*Mf*FcnA reveals enzyme subsite specificity and sulfated fucan substructural features

David Ropartz,[1,2,§] Lery Marion,[1,2,§] Mathieu Fanuel,[1,2] Jasna Nikolic,[3] Murielle Jam,[3] Robert Larocque,[3] Elizabeth Ficko-Blean,[3] Gurvan Michel,[3] Helene Rogniaux,[1,2,*]

1. INRAE, UR BIA, F-44316 NANTES, France

2. INRAE, BIBS facility, F-44316 NANTES, France

3. Sorbonne Université, CNRS, Integrative Biology of Marine Models (LBI2M), Station Biologique de Roscoff (SBR), F-29680 ROSCOFF, France

*Corresponding author: Helene.Rogniaux@inrae.fr

§ These authors contributed equally to this work

Running head: Detailed exploration of MfFcnA activity on sulfated fucans

Supplementary data items: **Table S1**: MzMine Software parameters used for the treatment of LC-MS. **Tables S2, S3 and S4**: complete list of oligofucans released at different reaction times with *Mf*FcnA; the species correspond to those plotted on Figures 2 and 3 of the main manuscript. **Figure S1**: C-PAGE profile of the digestion products by *Mf*FcnA of FCSPs originating from different sources. **Figure S2**: He-CTD spectra recorded for the DP4 and DP6 corresponding to the species: $(2.\text{Fuc} + 3.\text{S})_2$ and $(2.\text{Fuc} + 3.\text{S})_3$. **Figures S3, S4 and S5:** Postulated structures for, respectively, the most abundant pure fuco-oligosaccharides (from DP2 to DP6), the most abundant oligofucans containing one hexose (DP6, DP10 and DP12) and containing one pentose (from DP7 to DP13), as well as their possible production by *Mf*FcnA.

Keywords: Brown algae / GH107 / Mass spectrometry / *Pelvetia canaliculata* / Sulfated fucans

Abstract

The extracellular matrix of brown algae represents an abundant source of fucose-containing sulfated polysaccharides (FCSPs). FCSPs include sulfated fucans, essentially composed of fucose, and highly heterogeneous fucoidans, comprising various monosaccharides. Despite a range of potentially valuable biological activities, the structures of FCSPs are only partially characterized and enzymatic tools leading to their deconstruction are rare. Previously, the enzyme *Mf*FcnA was isolated from the marine bacterium *Mariniflexile fucanivorans* and biochemically characterized as an endo-α-1→4-L-fucanase, the first member of glycoside hydrolase family 107. Here, *Mf*FcnA was used as an enzymatic tool to deconstruct the structure of the sulfated fucans from *Pelvetia canaliculata* (Fucales brown alga). Oligofucans released by *Mf*FcnA at different time points were characterized using mass spectrometry coupled with liquid chromatography and tandem mass spectrometry through Charge Transfer Dissociation. This approach highlights a large diversity in the structures released. In particular, the analyses show the presence of species with less than three sulfates per two fucose residues. They also reveal species with monosaccharides other than fucose and the occurrence of laterally branched residues. Precisely, the lateral branching is either in the form of a hexose accompanied by a trisulfated fucose nearby, or of a side chain of fucoses with a pentose as the branching point on the polymer. Overall, the results indicate that the structure of sulfated fucans from *P. canaliculata* is more complex than expected. They also reveal the interesting capacity of *Mf*FcnA to accommodate different substrates, leading to structurally diverse oligofucan products that potentially could be screened for bioactivities.

1. Introduction

The extracellular matrix of brown algae represents a rich and abundant source of fucose-containing sulfated polysaccharides (FCSPs). FCSPs include two families of polysaccharides: sulfated fucans and fucoidans. Sulfated fucans are homopolymers of L-fucose displaying numerous substitutions (e.g. sulfate esters, acetyl groups), while fucoidans are heteropolymers containing sulfated L-fucose but whose main chains are constituted by various neutral and/or uronic monosaccharides (Deniaud-Bouët et al., 2017, 2014). The FCSPs extracted from brown algae are heterogeneous and their structure remains mostly uncharacterized. The majority of the available structural knowledge on brown algal FCSPs concerns sulfated fucans. In most Fucales species (including *P. canaliculata*), sulfated fucans have backbones containing long stretches of alternating α-(1→3) and α-(1→4)-L-fucose residues, bearing one sulfate group on the carbon at position C2 and/or C3 (Bilan et al., 2002; Chevolot et al., 2001; Colin et al., 2006) (**Figure 1**). In Laminariales, sulfated fucan backbones are only based on α-(1→3) linked L-fucose residues bearing one or two sulfate groups at C2 and C3 (Anastyuk et al., 2010; Nagaoka et al., 1999; Nishino et al., 1991; Sakai et al., 2003). As described by (Ale and Meyer, 2013) the structure of the polysaccharide strongly varies depending on the seaweed species. The backbone is also subject to modifications such as acetyl groups and/or sidechains of distinct lengths, as well as to variations in the bonding positions or changes in the sugar compositions (Yuguchi et al., 2016).

Because of their chemical diversity, FCSPs have an impressive range of biomedical activities, including anti-oxidative and anti-inflammatory properties (Deniaud-Bouët et al., 2017; Guerra Dore et al., 2013; Wang et al., 2019). However, the lack of in-depth knowledge of FCSPs structure and the scarce availability of enzymes leading to their deconstruction hamper the full exploitation of those properties. The first fucanase gene (*fcnA*) was cloned from the marine flavobacterium *Mariniflexile fucanivorans* (Barbeyron et al., 2008; Colin et al., 2006). Its corresponding gene product, referred to as *Mf*FcnA, was shown to be an endo-acting glycoside hydrolase and is the founding member of the GH107 family of the CAZy classification (http://www.cazy.org/) (Lombard et al., 2014). NMR analyses

of the major products released from the action of *Mf*FcnA, on the sulfated fucan from *Pelvetia canaliculata* (Fucales order) revealed that *Mf*FcnA specifically hydrolyses $\alpha(1\rightarrow4)$-glycosidic linkages within the repeating motifs [$\rightarrow$4)-α-L-fucopyranosyl-2,3-disulfate-(1$\rightarrow$3)-α-L-fucopyranosyl-2-sulfate-(1$\rightarrow$]n (Colin et al., 2006). The crystal structure of this endo-α-1,4-fucanase (EC 3.2.1.212) was recently determined, revealing a complex modular architecture (Vickers et al., 2018). The GH107 family catalytic module adopts a $(\alpha/\beta)_8$-barrel fold and its active site has an open groove topology, consistent with the endolytic character of *Mf*FcnA. The subsites -1 and +1 of *Mf*FcnA are respectively specific for L-fucopyranose-2-sulfate and L-fucopyranose-2,3-disulfate (Vickers et al., 2018). However, only the most abundant products have been successfully resolved in these two studies (Colin et al., 2006; Vickers et al., 2018), which is probably an incomplete view of the products actually released.

In this context, the present work used a highly sensitive approach based on ion-pair reversed-phase liquid chromatography (IP-RP-LC) hyphenated to high-resolution mass spectrometry (MS) in order to elucidate the low abundance products released by *Mf*FcnA from the sulfated fucan of *P. canaliculata*. This in-depth structural characterization intended to better describe the structure of sulfated fucans in Fucales. In secondary intention, it allowed to complete the structural knowledge on the substrate specificity of *Mf*FcnA. Hydrolysis kinetics were performed to highlight different potential deconstruction patterns. Some of the products were characterized by tandem MS (MS/MS), using an activation method based on an ion/ion interaction between ionized products and a highly energetic helium cations (Li and Jackson, 2017). This approach, called Helium charge transfer dissociation (He-CTD), has indeed proven to outperform the more conventional collision activated dissociation (CID) by efficiently fragmenting complex oligosaccharides and preserving labile modifications such as sulfations (Akoumany et al., 2019; Ropartz et al., 2017, 2016b).

2. Results

2.1 Enzymatic hydrolysis of sulfated fucans by *Mf*FcnA in MS-compatible conditions

Optimal condition for the activity of *Mf*FcnA was previously determined by Colin and coworkers to be the following: 20 mM Tris-HCl pH 7.5; temperature: 20°C (i.e., room temperature) (Colin et al., 2006).

However, the production of oligofucans in the above buffer would require a desalting step for subsequent MS analysis, which would cause possible loss of oligosaccharides. Therefore, ammonium bicarbonate was chosen as a buffer solution, since its volatility is compatible with mass spectrometry and its pH value (pH=8) with the enzymatic activity of *Mf*FcnA. The activity of *Mf*FcnA in 50 mM ammonium bicarbonate has been tested on sulfated fucans of *P. canaliculata*, as well as on sulfated fucans from other sources: the Fucales brown algae *Ascophylum nodosum* and *Fucus vesiculosus*, the Laminariales brown alga *Laminaria japonica* and the sea urchin *Paracentrotus lividus*. The C-PAGE profiles of the released oligofucans are provided in Supplementary Data (**Figure S1**). Under these conditions, the oligofucans released by *Mf*FcnA from *P. canaliculata* have a profile similar to that previously obtained in Tris-HCl buffer (Colin et al., 2006). As expected, *Mf*cnA is also active on the mixed-linked sulfated fucans from other Fucales (*A. nodosum* and *F. vesiculosus*) but is inactive on pure α-1,3-linked fucans (*L japonica* and *P. lividus*) (Berteau, 2003; Deniaud-Bouët et al., 2017).

2.2 Exploration of the oligofucans released at different digestion times by MfFcnA

The oligofucans from *P. canaliculata* released by *Mf*FcnA were analysed in depth by IP-RP-LC-MS. In order to explore the kinetics of the enzymatic reaction, four time points were chosen for the digestion: T=0H, 1H, 16H and 5 Days. The longer times of reaction (i.e., T=16H and 5 Days) aimed to maximise the degradation of the sulfated fucans by *Mf*FcnA, including cleavage of "non-ideal" patterns—in other words, not strictly composed of an alternation of [→4)-α-L-fucopyranose-2,3-disulfate-(1→3)-α-L-fucopyranose-2-sulfate-(1→] motif—that possibly exist in the heterogeneous polysaccharide. Thus, the aim was to increase the chemical diversity of the released oligofucans. The time point T=0H, in which the boiled enzyme was introduced with the sulfated fucans, was used as a control. As expected, no oligofucans were detected for T=0H (*data not shown*), meaning that all products detected for other time points were produced by the action of *Mf*FcnA.

With the aim to provide an efficient representation of the results, that keeps the comprehensiveness of the data while allowing an easy comparison of samples, results are presented in the form of graphs. The graphs plot the degree of sulfation (DS) divided by the degree of

polymerization (DP) (*i.e.*, DS/DP) as a function of the DP. This allows visualizing the oligosaccharide structures of a given family (in term of monosaccharide composition) independently of the sulfation degree. The surface area of the sphere in the graph is proportional to the ion intensity measured in MS for the different species, and has been normalized so that areas can be compared among graphs of a same figure. The complete list of the reaction products identified by MS is available in Supplementary Data **(Tables S2, S3 and S4)**. At this stage, structure assignment was made solely based on the mass measured for the molecular species and knowledge of the most common building blocks composing oligofucans (**Figure 1**). Eventual isomers have been grouped under the same bubble.

2.2.1 Ideal structural patterns among oligofucans

In a first step, we focused on the "ideal" structures described in the literature as composing the backbone of sulfated fucans from Fucales species, *i.e.*, a repeating unit of [→4)-α-L-fucopyranose-(1→3)-α-L-fucopyranose-(1→]. This is expected to lead to three possible disaccharide moieties (A-, B- or C-type) depending on the number of sulfates brought by the fucosyl residues, as represented in **Figure 1**. **Figure 2** displays the LC-MS results after 1H, 16H and 5 Days of degradation by *Mf*FcnA. All measured intensities of the plotted species are available in Supplementary Data, **Table S2**.

After one hour of enzymatic degradation, the major products correspond to oligosaccharides built from the ideal C-type moiety (2.Fuc + 3.S), with DP ranging from 4 to 20 (**Figure 2**). The most intense species corresponds to a molecule with 10 fucoses and 15 sulfates (DP of 10 and DS/DP of 1.5) and has a measured intensity of 1.67e6. This intensity accounts for about 30% of the total intensity measured for the oligofucans, after one hour of digestion with *Mf*FcnA. The ionic species detected in MS, at a mass-to-charge ratio (*m/z*) of 1296.12, was a triply charged ion of the type [M-15.H+12.HxA]$^{3-}$, where HxA stands for hexylammonium ($C_6H_{16}N^+$, 102.13 Da) and comes from the ion-pairing agent used for the LC separation. A very small amount of DP2 with DS/DP of 1.5 (pure C-type motif) was also detected (measured intensity of 3.38e3), as well as small amounts of oligofucans with DS/DP < 1.5 (DP4 to DP8, with an intensity of the magnitude order of 1e3), which likely derive from a combination of typical building blocks (for example, 1.B + 1.C leads to DP4 with DS/DP=1.25).

The structural patterns of the oligofucans released after 16H and after 5 Days are rather similar, but differ significantly from the situation at 1H. The species with a DS/DP = 1.5 have all shifted towards lower DPs. The major species now corresponds to a DP4, composed of two C-type moieties (*i.e.*, 4.Fuc + 6.S). The intensity of the DP2 species corresponding to the pure C-type motif notably increased and reached 4% of the total species after 5 Days. Finally, several species with more heterogeneity in terms of degree of sulfation became significantly present (all with DS/DP < 1.5). Some may correspond to pure motifs, although it cannot be excluded that they encompass a combination of other blocks. For instance, the DP8 with DS/DP =1 may arise from pure B-type pattern [(2.Fuc + 2.S)$_4$], but may also be formed by two A-type moieties and two C-type moieties [(2.Fuc + 1.S)$_2$-(2.Fuc + 3.S)$_2$]. Notably, no species could be detected corresponding to pure A-type pattern (2.Fuc + 1.S, DS/DP = 0.5) and most of the species detected can be explained by combining only B-type and C-type moieties. The species with a DP of 4 and a DS/DP of 1.75 contains 7 sulfates, necessitating that one moiety (2.Fuc) bears 4 sulfates, which does not correspond to an "ideal" block.

2.2.2 Oligofucans with divergent structures

Beyond the ideal moieties of A-, B- and C-type discussed above, the LC-MS analysis demonstrated the production, in the digested samples, of some oligofucans containing non-fucosyl residues. Precisely, these oligofucans contain glycoside residues whose masses correspond to regular hexosyl (i.e., not deoxyhexosyl) or to pentosyl residues. The interpreted results are presented in **Figure 3** for the three time points of the kinetics. **Supplementary Tables S3 and S4** provide the complete list of species with their measured intensities. The additional pentosyl or hexosyl residues have been included in the computation of the DP. Note that the species represented in **Figure 3**, on average, exhibit a 10-fold lower intensity than the "ideal" oligofucans represented in **Figure 2**. After 5 Days, the oligofucans bearing non-fucosyl residues represent 14% of the oligofucans released by *Mf*FcnA from *P. canaliculata* sulfated fucans.

At the time point T=1H (**Figure 3**), only a few species were apparent, all with a low intensity: two species bore one pentose, DP11 and DP13, while seven contained an additional hexose other than

7

fucose, DP6, DP10 and DP12. Two of the identified species with one hexose have a DS/DP between 1.2 and 1.5. For instance, the species of DP10 with a DS/DP of 1.5 encompass 9.Fuc + 1.Hex + 15.S. In other words, this species could fit with five C-type blocks, in which the hexose would replace the fucose in one block and bear one to two sulfate groups. Species that contain a pentose are less sulfated (DS/DP < 1.2). At T=16H, more species containing hexose or pentose in the oligofucans appeared, in the range of DP6 to DP14.These species had increased intensity compared to the 1H time point, especially those corresponding to the less sulfated species (DS/DP < 1.4). Conversely, the species which contain one hexose and a higher DS/DP (between 1.4 and 1.5) remained more or less stable in intensity between T=1H and T=5 Days. For the products containing a pentose, the species identified at T=1H showed an enhanced intensity and many species with low sulfation degrees emerged (DS/DP < 1.1). At T=5 Days, intensities of the released products from both families (hexose or pentose) did not evolve compared to T=16H, with the exception of two species of DP10 (DS/DP = 1.3 and DS/DP = 1.2). Interestingly, all species with one hexose exhibit an even DP while all species with one pentose exhibit uneven DPs and relatively low DS/DP ratios.

In the next stage, a deeper characterization of selected representative structures of oligofucans produced by *Mf*FcnA was performed using He-CTD MS/MS.

2.3 Structural study of released oligofucans

In order to determine the exact structure of some oligofucans and refine the substrate specificity of *Mf*FcnA, four representative structures produced from *Mf*FcnA digest of sulfated fucans were structurally studied by He-CTD MS/MS, without and with ^{18}O-labelling of the reducing end, as well as in positive and negative ionisation modes. The ^{18}O-labelling specifically targets the hydroxyl group at the reducing end of the oligosaccharide. It intends to break the glycoside symmetry and thus, leads to the differentiation of the non-reducing and reducing ends isobaric fragments (since all reducing end fragments will be shifted by 2 Da). This strategy allows for directional sequencing of the oligosaccharides and thereby, is a means of consolidating the interpretation of the fragments observed and of assembling the full-length oligosaccharide structure. Only the results obtained on the [18]O-

labelled structures in positive ionisation mode are presented. MS/MS fragmentation by He-CTD is favoured for its ability to obtain an extended fragmentation of oligosaccharides above DP8 and, importantly, to preserve labile functions—including sulfate groups—as established previously in our group (Akoumany et al., 2019; Ropartz et al., 2017, 2016b). The latter is a key point for the structural analysis of complex sulfated carbohydrates, such as those in algae, which overcomes the limitation of collisionally induced MS fragmentation (CID) (Ropartz et al., 2016b).

Four selected candidates for He-CTD MS/MS investigation were chosen. Two from the oligofucans composed of pure C-type moieties in order to confirm those structures, which have been previously characterized by NMR (Colin et al., 2006; Vickers et al., 2018). Two from the oligofucans exhibiting a pentose or a regular hexose (i.e., a non deoxy-hexose), to investigate whether these monosaccharides are found in the backbone or on lateral branch points and if they bear a sulfate group.

Concerning the C-type structural patterns, we isolated one DP4 (4.Fuc + 6.S) as $[M-6.H+8.HxA]^{2+}$ ion at m/z 947.5, and one DP6 (6.Fuc + 9.S) as $[M-9.H+11.HxA]^{2+}$ ion at m/z 1365.2. **Figure 4** gives the structures that could be deduced for both DPs from the He-CTD spectra, with an annotation of the fragments that led to unambiguously establish those structures (the spectra are available in Supplementary Data, **Figure S2**). For the DP4, we obtained a complete series of $^{1,5}X_n$, Y_n and Z_n and of C_n and B_n fragments. The Y_n and Z_n fragments, which contain the reducing end, were shifted by 2 Da due to the heavy oxygen labelling and could thus be differentiated from possible isobaric B_n and C_n fragments. For the DP6, the fragmentation pattern was less comprehensive than for the DP4. However, at least one specific fragment could be identified between each subunit. In both cases, the reducing end consisted of a mono-sulfated fucosyl residue while a di-sulfated fucose was found at the non-reducing end. The result showed a strict alternation between mono- and di-sulfated fucoses along the backbone. Thus, the fragmentation profiles of both oligosaccharides were in agreement with the ideal pattern of C-type disaccharides, as well as with the expected enzyme specificity, described as cleaving the α(1→4)-glycosidic linkages within the repeating motifs [→4)-α-L-fucopyranosyl-2,3-disulfate-(1→3)-α-L-fucopyranosyl-2-sulfate-(1→]n (Colin et al., 2006).

The next representative structure of oligofucans released by *Mf*FcnA that was selected for a deeper structural investigation by He-CTD was a DP6 bearing one hexose (5.Fuc + 1.Hex + 8.S). It was isolated as $[M-8.H+10.HxA]^{2+}$ ion at *m/z* 1282.6. **Figure 5** shows the fully interpreted He-CTD spectrum as well as the annotated structure. For clarity, only the specific fragments discussed below were annotated on the structure. The fragmentation spectrum highlighted different interesting features. Considering the $^{1,5}X_1$ (*m/z* 477.2) and Y_1 *(m/z* 449.2), it could be deduced that the structure has a mono-sulfated fucose at the reducing end. From the other end, two ions (*m/z* 628.1 and *m/z* 610.1) were identified as C_1 and B_1 fragments and placed a di-sulfated fucose residue at the non-reducing end. Two fragments at *m/z* 809.2 and 791.2 were found to be specific of this species (*i.e.,* not measured for the C-type structures solved before). Their masses correspond to a trisulfated fucose with four HxA counter-ions. These ions did not shift upon ^{18}O labelling, which indicates that they do not include the reducing end. In parallel, the ^{18}O-labelled fragments at *m/z* 1447.5 and 1463.6, attributed respectively to a Z_2 and Y_2'' fragments, included the trisulfated fucose while the Y_1 fragment (*m/z* 449.2) did not. The mass difference between these two series correspond to two fucoses, four sulfates and four HxA. Overall, these fragments positioned a trisulfated fucose as a laterally branched moiety on the second residue from the reducing end. One sulfate group is found as well on the same fucosyl residue. Nonetheless, the exact positioning of the trisulfated fucose and of the sulfate group remains uncertain (either C2 or C3). The two fragments at *m/z* 809.2 and 791.2 were indicated with a Greek letter α in the mass spectrum (C_α and B_α, respectively).

Concerning the hexose, a set of fragments lead us to propose that the hexose is laterally branched on the second residue from the non-reducing end (**Figure 5**). These fragments are the following: *m/z* 1116.5 (2.Fuc + 3.S + 1.Hex + 4.HxA) and *m/z* 628.1 (1.Fuc + 2.S + 3.HxA). Both contain the non-reducing end, as they do not shift upon ^{18}O-labelling, and were interpreted as C_2 and C_1 fragments. In accordance with the proposed structure, losses of 162 Da (corresponding to the loss of a hexose) are clearly visible on the mass spectrum from C_2 (and also C_3) but not from C_1. The *m/z* 1953.8 (4.Fuc + 6.S + 1.Hex + 7.HxA) and the corresponding doubly-charged ion at *m/z* 1028.4, and the *m/z* 1463.6 (3.Fuc + 5.S +

6.HxA) were interpreted as $Y_3^\bullet$, Y_3^{2+} and Y_2'' and all corroborated the above hypothesis; in particular, a loss of 162 Da was observed for Y_3^{2+} but not for Y_2''. For clarity, the complementary Z and B fragments were not mentioned above although they were observed on the mass spectrum and confirmed the proposed structure. Notably, the concomitant observation of 162 Da losses from the m/z 1936.8 (Z_3) and m/z 1116.5 (C_2) cannot be explained if the hexose is in the backbone. Due to significant noise in the low mass region, the He-CTD acquisition started at m/z 300 and thus, the m/z 282.2 corresponding to [1.Hex + 1.HxA]$^+$ could not be detected. The interpreted fragments leaves an ambiguity on the exact positioning of the hexose, either on the C2 or on the C4 of the second fucosyl residue from the non-reducing end.

The last structure selected for fragmentation was a DP9 oligofucan with one pentose (8.Fuc + 1.Pen + 8.S), isolated as [M-8.H+10.HxA]$^{2+}$ ion at m/z 1486.76. **Figure 6** shows the fully interpreted He-CTD spectrum as well as the annotated structure. The $^{1,5}X_1$ (m/z 477.2), Y_1 (m/z 449.2) and Y_2 (m/z 957.5), demonstrate the presence of a classical C-type moiety at the reducing end (α-L-fucopyranose-2,3-disulfate-(1$\rightarrow$3)-α-L-fucopyranose-2-sulfate). The C_5^{2+} and B_4 fragments (respectively at m/z 1323.2 and m/z 1914.6) validate this part of the structure. Considering the series of B fragments, B_3 (m/z 1587.6) and B_2 (m/z 1260.6) show that the third and fourth residues from the reducing end correspond to two singly sulfated fucans, thus typically a B-type block. On the other end of the structure, two doubly charged fragments ($Y_5^{2+/\bullet}$ at m/z 1232.5 and Z_5^{2+} at m/z 1223.6) and two singly charged fragments (C_1 at m/z 628.4 and B_1 at m/z 610.4) indicate the presence of a doubly sulfated fucose at the non-reducing end. This leaves three fucoses, one pentose and one sulfate group to be positioned in-between this fucosyl residue and the "B-type block – C-type block" sequence of the reducing end. Two fragments, at m/z 725.2 and m/z 707.4, were found to be specific of this structure (*i.e.*, not observed in the He-CTD spectra of other structures). These fragments match with the singly-charged trisaccharide: [2.Fuc + 1.S + 1.Pen + 1.HxA]$^+$. Our hypothesis is that this chain is branched laterally on the second fucose residue from the non-reducing end, which led us to annotate the aforementioned fragments as being C_α and B_α. This interpretation is corroborated by the observation

of the fragments at *m/z* 1918.5, 1428.5, 1101.6, 1083.5, 774.4, 766.4, which all fit with a loss of 605.2 Da (corresponding to 2.Fuc + 1.S + 1.Pen + 1.HxA) from the B_5, C_4, C_3, B_3, C_2, B_2 ions respectively. In addition, the Y_5 fragment, detected at *m/z* 1232.5 as a doubly charged ion, exhibited a loss of 605.2 Da, as evidenced by the singly charged fragment at *m/z* 1656.9. The exact positioning of the trisaccharidic lateral chain may be on the C2 or C4 position of the fucosyl subunit.

3. Discussion

The present work provides an in-depth structural characterization of the oligosaccharide products released by *Mf*FcnA from sulfated fucans extracted from *P. canaliculata.* The primary goal of this study was to improve the structural knowledge of sulfated fucans in Fucales. In secondary intention, our results allowed to refine the fine substrate specificity and mode of action of *Mf*FcnA, first member of the GH107 family. The study was performed at different kinetics time points: from 1H to 5 Days. Longer kinetics aim to promote the degradation of the polymer, including that of non-preferential patterns. At short times of reaction (T=1H), *Mf*FcnA produces a majority of oligosaccharides with a DS/DP of 1.5, which fit with the pure C-type motif (α-L-fucopyranose-2,3-disulfate-(1→3)-α-L-fucopyranose-2-sulfate). These species represent 99% of the released oligofucans at 1H. When the reaction goes further (T=16H and more), the prominent product in the mixture is the DP4 with a DS/DP=1.5, corresponding to two C-type units. This structure was also the major product found in previous studies using NMR (Colin et al., 2006; Vickers et al., 2018). It confirms the strong preference of *Mf*FcnA for cleaving the α-(1→4)-glycosidic linkage within repeating motifs of the type: [→4)-α-L-fucopyranosyl-2,3-disulfate-(1→3)-α-L-fucopyranosyl-2-sulfate-(1→]n. The main oligofucan species produced by *Mf*FcnA (referred to as "classical species") contain 47 % (w/w) of sulfate groups, which is in agreement with previous results (Colin et al., 2006). Previous research on intact fucans from *P. canaliculata* have shown that different fucan fractions from this species contain between 29-40 % (w/w) of sulfate groups (Descamps et al., 2006; Mabeau et al., 1990; Ponce and Stortz, 2020). Thus, the main oligofucan species produced by *Mf*FcnA are significantly more sulfated compared to the intact fucan fractions. This suggests that *Mf*FcnA degrades in priority the highly sulfated domains in the sulfated fucan chain.

The sensitivity of the analytical method employed in the present study, as well as its capacity of resolving a high molecular complexity, revealed a much wider chemical diversity of products released by *Mf*FcnA, especially for longer times of reaction. Our analyses revealed a variety of oligofucans that do not match with pure C-type motifs (DS/DP < 1.5). Overall, these species contribute to a significant proportion of the released products, representing approximately 25% of the oligofucan products after 5 Days of degradation. Most of them can be explained by combining C- and B-type blocks, although a contribution of A-type block cannot be excluded. Notably, many species are less sulfated in comparison to pure C-type motifs (i.e., they contain less than three sulfate per two fucose residues), suggesting a tolerance of *Mf*FcnA for substrates with lower sulfation degrees. Mass spectrometry is known to promote desulfation in the gas phase. However, this effect is reduced here thanks to the protecting effect of the ion-pairing reagent (HxA) which binds to each sulfate group. Also, species differing by their sulfation status exhibited different retention times in LC, which proves that the difference in their number of sulfates was not induced by the mass spectrometry process.

One striking result of this study concerns the complex, branched structures, which were evidenced among the released oligofucans. These structures are not composed solely of sulfated fucoses, i.e., of deoxyhexoses. Their mass indicates that they also include either one pentose or one "regular" hexose. These species were mostly produced after long reaction times with *Mf*FcnA (T=16H and longer). Even if they exhibit a lower abundance than the pure fucose-containing oligosaccharide products (about 10 to 50-fold on average), they are diverse in terms of DP and DS and are significantly represented in the reaction medium. Indeed, they account for 5% and 9% and of the oligofucans released by *Mf*FcnA after 5 Days, for the pentose and "regular" hexose containing species, respectively. The presence of hexoses (Gal and Man) and pentoses (Xyl), was corroborated by a compositional analysis of the starting material and represents around 20% in dry weight (*data not shown*). It also agrees with previous research on *P. canaliculata* sulfated fucans. Notably, intact sulfated fucans contained 81% Fuc, 9% Xyl, 7% Gal, 2% Man and 1% Glc (Mabeau et al., 1990). The oligofucans released by the extracellular enzymatic fraction from *M. fucanivorans* contained about 84% Fuc, 6% Xyl, and

10% Gal, as well as traces of Man and Glc (Descamps, 2006). These data suggest that the hexose detected in the present study corresponds most likely to Gal, while the detected pentose corresponds to Xyl, which is the only pentose found so far in *P. canaliculata* sulfated fucans (Descamps et al., 2006; Mabeau et al., 1990).

Interestingly, all species bearing one hexose display even DPs, whereas species bearing one pentose have odd DPs. Furthermore, the oligosaccharides bearing one hexose have higher DS/DP than the ones bearing one pentose. *Prima facie*, this initially suggested that the pentose might be a non-sulfated laterally branched residue, whereas the hexose might replace one of the fucosyl residues in the backbone and be sulfated. The structural examination of two selected structures using He-CTD tandem MS has discarded this interpretation. In fact, both the hexose and the pentose are branched laterally on the fucosyl main chain. The hexose was established as a single residue branched on a mono-sulfated fucose (**Figure 5**). The pentose was found to be part of a longer trimeric chain, which comprises two fucosyl residues along with one pentose (**Figure 6**). This trisaccharide branched on the backbone leads to an oligosaccharide of uneven DP. Another finding of these structural analyses is the existence, in the hexose-containing species, of a trisulfated fucosyl residue branched laterally on a nearby backbone fucose (**Figure 5**). The two laterally linked residues (*i.e.*, the hexose and the trisulfated fucose) restore parity in the number of residues, leading to even DPs of hexose-containing oligofucans. The occurrence of such trisulfated fucose has been evidenced in the context of fucoidans isolated from the brown alga *Saccharina latissimi* (formerly *Laminaria saccharina*) (Bilan et al., 2010).

Overall, our results suggest a much wider tolerance of *Mf*FcnA than previously described (Colin et al., 2006; Vickers et al., 2018). The large amount of DP4 produced (4.Fuc + 6.S) leads us to propose that the active site of *Mf*FcnA is symmetric and comprises eight subsites. This hypothesis is consistent with the length and the topology of the active site identified in the crystal structure of *Mf*FcnA (Vickers et al, 2018). Also, there seems to be a strong constraint for a pure C-type motif in subsites -1/-2 and +1/+2 as all the species produced with a DP of 4 have at least one C-type moiety. This finding agrees with the specificity of subsites -1 and +1 of *Mf*FcnA for L-fucopyranose-2-sulfate and L-fucopyranose-2,3-

disulfate, as described earlier (Vickers et al., 2018). Subsites -3/-4 would have tolerance for less-sulfated moieties while subsites +3/+4 could be left empty. This corresponds well with the observation of a DP4 with a DS/DP=1.25, which would correspond to a "B-type block – C-type block" sequence, as well as with the observation of the DP2, which is produced only as a pure C-type unit. The above hypothesis on the subsite tolerance of *Mf*FcnA fits well, for instance, with all the DP6 oligofucans observed in **Figure 2**. The DP6 with DS/DP=1.5, which is made of pure C-type units, would place a C-type block in subsites -1/-2 and a C-type unit in subsites -3/-4 (Supplementary Data, **Figure S3**). The DP6 with DS/DP=1.33 (8.S), which fits with two C-type blocks and one B-type block, would have the C-type block in subsites -1/-2, and either a B- or a C-type unit in subsites -3/-4. The DP6 with DS/DP=1.17 (7.S), which fits with two B-type blocks and one C-type block, would have a C-type block in subsites -1/-2 and a B-type block in subsites -3/-4. Finally, the DP6 with DS/DP=1 (6.S), which fits with one A-, one B- and one C-type block, would have the C-type block occupying subsites -1/-2 while the B block would be in subsites -3/-4. A synthesis of the above discussion about *Mf*FcnA subsites is presented in **Figure 7**.

Considering the oligofucan structures containing one hexose, the DP10 forms are produced first (T=1H) and become prominent at longer times of reaction (T=16H and longer). They represent 56% of the oligofucans with one hexose after 5 Days. From the structure resolved by tandem MS for the DP6, we postulate the following structure for the most abundant species (DP10, 12.S) from the non-reducing end: one C-type block with a laterally branched hexosyl residue, one A-type block with a laterally branched trisulfated fucose, one B-type block and one C-type block (Supplementary Data, **Figure S4**). This would place the C-type unit in subsites -1/-2 and a B-type block in subsites -3/-4. This structure makes any further degradation by *Mf*FcnA difficult, which fits with the fact that it becomes the prominent product after 16 hours of reaction. The DP8 species, which are detected after longer reaction times (T=16H and longer) and with lower abundance (they account for 8% of the oligofucans with one hexose after 5 Days), are relatively more sulfated (9.S, 10.S, 11.S; DS/DP of 1.12, 1.25 and 1.37, respectively) compared to the DP10. One hypothetical structure of the DP8 with 10 sulfates,

which fits with the subsites specificities of *Mf*FcnA, is proposed in **Figure S3.** This structure could arise from a DP12 (16.S) from a cleavage between two C-type moieties. The DP6 (8.S), which has been resolved structurally by He-CTD MS, suggests that the trisulfated fucose, and possibly the fucosyl with a lateral hexose, could be accommodated in the active site of *Mf*FcnA (Supplementary Data, **Figure S4**). However, these DP6 species are much less abundant than the DP10 or DP8 described above.

Finally, the species bearing one pentose are detected after longer reaction times. They remain at a stable but relatively low abundance between T=16H and 5 Days. Altogether, these species represent 5% of the oligofucans released by *Mf*FcnA after 5 Days. The smaller DP observed for these species is a DP7. In contrast to the structure resolved for the DP9, in which the pentose was linked to the fucosyl backbone as part of a trimeric chain (see **Figure 6**), structural analysis of the DP7 showed branching of the pentose as a single residue on the backbone (*data not shown*). We postulate that the pentose-containing species that are detected in **Figure 3** share a backbone of six to eight fucosyl residues. The pentose is linked directly to the second fucosyl residue from the non-reducing end of the oligofucan either as a single residue, or as part of a longer chain. The different DPs observed in **Figure 3** would arise from this lateral chain elongating by further addition of di-fucosyl blocks (*i.e.*, 0 for DP7, 1 block for DP9, 2 blocks for DP11) (Supplementary Data, **Figure S5**). All the species detected with one pentose can be rationalized considering the subsite specificities proposed for *Mf*FcnA in **Figure 7**. Precursors are sulfated fucans with a side chain containing the pentose, the pentose being the branching point. The side chain can be relatively short and composed of A-type, B-type or C-type di-fucosyl units (Supplementary Data, **Figure S4**). It could also be much longer and itself constitute another polysaccharide chain. In any case, our data suggests that the side chain containing the pentose must be located at the non-reducing end of the precursor polymer.

In conclusion, a fine structural analysis on the products released from the sulfated fucans of *P. canaliculata* by the endo-α-1,4-fucanase *Mf*FcnA, the first characterized member of the GH107 family, has been undertaken. The analytical strategy used mass spectrometry coupled with ion-pair reversed-phase liquid chromatography (IP-RP-LC) and tandem MS by Helium-Charge Transfer Dissociation (He-

CTD). This very sensitive and comprehensive approach revealed greater complexity in the structures released by *Mf*FcnA than the expected strict alternation of ideal patterns, consisting of single and double sulfated fucosyl residues (Colin et al., 2006; Vickers et al., 2018). In particular, the analyses showed the presence of glycosyl-residues other than fucose in the reaction products; more precisely, we found oligofucans containing either one hexose (probably Gal or Man) or one pentose (probably Xyl). Structural determination demonstrated a lateral branching for these non-fucosyl residues. The hexosyl residue is always found with a neighbouring trisulfated fucose, which could suggest that this motif serves a signalling function for the alga. The pentose appears to be the branching point of a lateral chain made of sulfated fucoses. Our data suggests that this chain is located at the non-reducing end of the polymer and we hypothesize it develops as a fucan chain itself.

The heterogeneity found in sulfated fucans of *P. canaliculata* agrees with some recently published extensive analyses of the composition of sulfated fucans from brown algae of the order Fucales (Ponce and Stortz, 2020). The specialized fucan structures discovered in the present study contribute to the complexity of the polymer and are likely important in protection against degradation by marine microbial pathogens. In addition, our study revealed the interesting ability of *Mf*FcnA to recognize different patterns within sulfated fucans. This flexibility suggests an adaptation of marine bacteria to the significant heterogeneity of sulfated fucans. The result, as shown here, is the release of structurally diverse oligofucans that potentially could be screened for bioactivities.

4. Materials and Methods

a. Chemicals

Hexylamine 99% (HxA) was purchased from Sigma-Aldrich Co. (Saint Quentin Fallavier, France). Acetic acid 98% was from Fluka (purchased by Sigma-Aldrich Co., Saint Quentin Fallavier, France). HPLC-grade acetonitrile (ACN) was purchased from Carlo-Erba Reagents (Val de Reuil, France). Ultrapure water was obtained from a Milli-Q apparatus (Millipore).

b. Preparation of sulfated fucans from *P. canaliculata*

Multiple individuals of *P. canaliculata* were collected from rocky shore of Moguériec, France. Collected algae were washed with tap water, and dried overnight at 50°C. Dry algal material (430 g) was milled into powder. Afterwards, alcohol insoluble residue (AIR) was prepared according to the modified protocol by Salmeán and coworkers (Salmeán et al., 2018). AIR was soaked during 75 min at RT in water acidified with H_2SO_4 (pH 2.9) (1:15, w/v). Sulfated fucans extraction and purification were performed according to the modified protocol by Kloareg and co-workers (KLOAREG et al., 1979). Briefly, extraction was done for 30 min at 98°C under mechanical stirring. Raw algal extract was centrifuged (30 min, 14000 g, RT), and the supernatant was collected. Remaining precipitate was used for one re-extraction, and the raw re-extract was clarified under the same conditions. Raw extract and re-extract were treated separately. The pH was adjusted to 6.25, and co-extracted alginate was precipitated by the addition of 2M $CaCl_2$ to a final concentration of 2% $CaCl_2$ (w/v). Alginate was removed by centrifugation (20 min, 14000 g, RT) and the supernatant was collected. Cold 96 % (w/w) ethanol was added to obtain a final ethanol concentration of 70% (w/w) and left overnight at 4°C. Precipitated sulfated fucans were pelleted by centrifugation (20 min, 14000 rpm, 4°C). The pellet was solubilized in a minimal volume of water and dialyzed against water using CO 12-14 kDa (Sigma Aldrich) to remove remaining salts, oligosaccharides and any low-molecular weight compounds. Desalted samples were freeze-dried. The sulfated fucans from the first extraction and the re-extraction were denoted as E and R fractions, respectively. The current study used the sulfated fucans from the R fraction only.

c. Cloning and overproduction of the recombinant endo-fucanase *Mf*FcnA

For production of *Mf*FcnA, the *fcnA* gene (Colin et al., 2006) was cloned as described by Groisillier and coworkers (Groisillier et al., 2010) using the forward primer AAAAAAAGATCTCAAGTACCAGATCCAAACCAAGGA and the reverse primer TTTTTTCAATTGTTAATTTCCATCACTAATAATAGTTGCAATT. Plasmid DNA was transformed into *Escherichia coli* BL21 (DE3) expression strain. Protein production was done at 20°C in 1 L of auto-induction ZYP 5052 medium (Studier, 2005) supplemented with 100 μg/ml ampicillin. Cells were

harvested after 72 hours by centrifugation (15 min, 8000 g, 4˚C). Cell harvesting was followed by chemical lysis (Ficko-Blean et al., 2015). Clarified cell lysate was loaded onto an immobilized metal-affinity chromatography (IMAC) column (5 ml His Trap GE Healthcare) and unbound protein fraction was removed by washing with binding buffer (20 mM Tris–HCl, 500 mM NaCl, 20 mM Imidazole, pH 7.6). Bound proteins were eluted using a linear gradient 0 to 100 % of elution buffer (20 mM Tris–HCl, 500 mM NaCl, 500 mM Imidazole, pH 7.5). Collected *Mf*FcnA purified protein fractions were pooled and further purified by size-exclusion chromatography (125 ml Superdex 200) using an isocratic gradient (20 mM Tris–HCl, 500 mM NaCl, pH 7.5). Purity of the protein was confirmed by SDS PAGE analysis on a 12 % polyacrylamide gel.

d. Hydrolysis of sulfated fucans using *Mf*FcnA

Prior to enzymatic digestion, the purification buffer solution of *Mf*FcnA was exchanged against 50 mM ammonium bicarbonate using Amicon ultra device (cut-off at 30 kDa). Digestions of 2 % (w/v) fucans from *P. canaliculata*, *A. nodosum* (Elicityl, France), *F. vesiculosus* (Elicityl, France), *L. japonica* (Carbosynth, UK) and *P. lividus* (gift from Prof. Patrick Cormier, Station Biologique de Roscoff, France) were done overnight (16H) in 50 mM ammonium-bicarbonate at room temperature (R.T., 20˚C). *Mf*FcnA concentration in each of the reaction mixtures was 0.05 mg/mL. Following the digestion, 1 µL of each digestion mixture was applied onto carbohydrate polyacrylamide gel electrophoresis (C-PAGE) according to the protocol of Zablackis and Perez (Zablackis and Perez, 1990), with 4 % stacking and 27 % resolving polyacrylamide gels. For mass spectrometry analyses, digestions of 2 % (w/v) fucans from *P. canaliculata* (R fraction) were done in 50 mM ammonium bicarbonate at 20 °C (R.T.). *Mf*FcnA concentration in the reaction mixture was 0.05 mg/mL. Released products were recovered at different times: T=0H corresponds to incubation with the boiled enzyme; 1H; 16H; and 5 Days. Enzymatic digestions were stopped using thermal denaturation (10 min at 95°C).

e. Heavy oxygen labelling of oligofucans

Prior to tandem MS experiments, samples at 0.2% (w/v) in 50 mM ammonium bicarbonate were vacuum dried at room temperature in using a speed vacuum concentrator system. The reducing ends

of the oligosaccharides were ^{18}O-labeled by suspending the dried material in 50 µL of $H_2^{18}O$. Incubation was allowed for one week at 70°C, in the dark.

   f. UHPLC-MS analyses of the oligofucans

Ion-pair reversed-phase (IP-RP) separation was run on an ultrahigh performance liquid chromatography system (UHPLC, Acquity H-Class plus® Waters, Wilmslow, UK), equipped with a BEH C18 column (100 mm x 1 mm, packed with 1.7 µm porosity particles) (Waters, Wilmslow, UK). The flow rate was 0.15 mL.min^{-1} and the column was heated at 45°C. A ternary gradient was used with A, pure water; B, pure acetonitrile; and C, 20 mM HxA dissolved in water (pH value adjusted to 6 by addition of acetic acid). The gradient was from 16.6% to 35% of solvent B in 10 min, then up to 63.4% at 20 min and maintained at 73.4% for 4.5 min. Solvent C was kept constant at 25% (Ropartz et al., 2016a).

Acquisitions were performed through direct coupling of the UHPLC system with a Select Series Cyclic IMS mass spectrometer (Waters, Wilmslow, UK) (Giles et al., 2019). Spectra were acquired in negative electrospray ionization (ESI) mode on the m/z range 300 – 2000, with the TOF (Time-of-flight) analyser operating in the V-mode. The source parameters were the following: Capillary voltage 2.5 kV; Cone Voltage: 40V; Source temperature: 100°C; Desolvation temperature: 280°C; Desolvation gas: 500 L/hour; Nebulization gas: 5.5 bar. Data were recorded with the Quartz software (Waters embedded software, release 5) and processed using Mass Lynx 4.2 (from Waters, Wilmslow, UK) and MzMine software (Pluskal et al., 2010). MzMine was used to produce a database of annotated structures (m/z; retention time; intensity) that can be exported in a tabulated format. Parameters used in MzMine are described in the Supplementary Data, **Table S1**.

   g. He-CTD MS/MS analysis of the oligofucans

The ^{18}O-labeled samples were diluted 4-fold in a solution of $H_2^{16}O$/20 mM HxA pH6 in $H_2^{16}O$ /ACN (1:1:2, in volume) right before the analysis. Helium-Charge Transfer Dissociation (He-CTD) spectra were obtained on a modified AmaZon 3D ion trap (Bruker Daltonics, Billerica, MA, USA) with helium as the CTD reagent gas as described by Ropartz et al. 2017 (Ropartz et al., 2017). Doubly charged precursor ions were isolated in positive mode using an isolation window of 6 Da. Ion accumulation times were

set at 10 ms. The CTD beam at 6 kV was pulsed during 100 ms per scan. Data were recorded for 5 min, over m/z range of 300 – 2200. The sample were infused at a flow rate of 10 µL/min. Raw data were converted into mzML format using MSConvert and processed with mMass 5.5.0 (Niedermeyer and Strohalm, 2012). Peak picking was performed using a signal-to-noise threshold of 5 and a minimum relative intensity of 1%. Fragment peaks were annotated according to the nomenclature of Domon and Costello (Domon and Costello, 1988).

5.   Acknowledgements

Author contributions

6.   ORCID identifications

D. Ropartz: 0000-0003-4767-6940

L. Marion: 0000-0002-7003-4404

M. Fanuel: 0000-0001-8384-8266

J. Nikolic: 0000-0002-0169-1507

M. Jam: 0000-0002-9357-5676

E. Ficko-Blean   0000-0002-3915-4715

G. Michel: 0000-0002-3009-6205

H. Rogniaux: 0000-0001-6083-2034

7.   Abbreviations

DS: degree of sulfation. DP: degree of polymerization. FCSP: fucose-containing sulfated polysaccharides. Fuc: Fucose. S: Sulfate; Hex: Hexose. Pen: Pentose. Gal: galactose. Man: mannose. Xyl: Xylose. HxA: hexylammonium.

8. Data availability statement

Data can be made available by the authors on request to the corresponding author.

9. References

Akoumany, K., Zykwinska, A., Sinquin, C., Marchand, L., Fanuel, M., Ropartz, D., Rogniaux, H., Pipelier, M., Delbarre-Ladrat, C., Colliec-Jouault, S., 2019. Characterization of New Oligosaccharides Obtained by An Enzymatic Cleavage of the Exopolysaccharide Produced by the Deep-Sea Bacterium Alteromonas infernus Using its Cell Extract. Molecules 24, 3441. https://doi.org/10.3390/molecules24193441

Akoumany, Zykwinska, Sinquin, Marchand, Fanuel, Ropartz, Rogniaux, Pipelier, Delbarre-Ladrat, Colliec-Jouault, 2019. Characterization of New Oligosaccharides Obtained by An Enzymatic Cleavage of the Exopolysaccharide Produced by the Deep-Sea Bacterium Alteromonas infernus Using its Cell Extract. Molecules 24, 3441. https://doi.org/10.3390/molecules24193441

Ale, M.T., Meyer, A.S., 2013. Fucoidans from brown seaweeds: an update on structures, extraction techniques and use of enzymes as tools for structural elucidation. RSC Adv 3, 8131–8141. https://doi.org/10.1039/C3RA23373A

Anastyuk, S.D., Shevchenko, N.M., Nazarenko, E.L., Imbs, T.I., Gorbach, V.I., Dmitrenok, P.S., Zvyagintseva, T.N., 2010. Structural analysis of a highly sulfated fucan from the brown alga Laminaria cichorioides by tandem MALDI and ESI mass spectrometry. Carbohydr. Res. 345, 2206–2212. https://doi.org/10.1016/j.carres.2010.07.043

Barbeyron, T., L'Haridon, S., Michel, G., Czjzek, M., 2008. Mariniflexile fucanivorans sp nov., a marine member of the Flavobacteriaceae that degrades sulphated fucans from brown algae. Int. J. Syst. Evol. Microbiol. 58, 2107–2113. https://doi.org/10.1099/ijs.0.65674-0

Berteau, O., 2003. Sulfated fucans, fresh perspectives: structures, functions, and biological properties of sulfated fucans and an overview of enzymes active toward this class of polysaccharide. Glycobiology 13, 29R – 40. https://doi.org/10.1093/glycob/cwg058

Bilan, M.I., Grachev, A.A., Shashkov, A.S., Kelly, M., Sanderson, C.J., Nifantiev, N.E., Usov, A.I., 2010. Further studies on the composition and structure of a fucoidan preparation from the brown

alga Saccharina latissima. Carbohydr. Res. 345, 2038–2047.

https://doi.org/10.1016/j.carres.2010.07.009

Bilan, M.I., Grachev, A.A., Ustuzhanina, N.E., Shashkov, A.S., Nifantiev, N.E., Usov, A.I., 2002.

Structure of a fucoidan from the brown seaweed Fucus evanescens C.Ag. Carbohydr. Res.

337, 719–730. https://doi.org/10.1016/S0008-6215(02)00053-8

Chevolot, L., Mulloy, B., Ratiskol, J., Foucault, A., Colliec-Jouault, S., 2001. A disaccharide repeat unit

is the major structure in fucoidans from two species of brown algae. Carbohydr. Res. 330,

529–535. https://doi.org/10.1016/S0008-6215(00)00314-1

Colin, S., Deniaud, E., Jam, M., Descamps, V., Chevolot, Y., Kervarec, N., Yvin, J.-C., Barbeyron, T.,

Michel, G., Kloareg, B., 2006. Cloning and biochemical characterization of the fucanase FcnA:

definition of a novel glycoside hydrolase family specific for sulfated fucans. Glycobiology 16,

1021–1032. https://doi.org/10.1093/glycob/cwl029

Deniaud-Bouët, E., Hardouin, K., Potin, P., Kloareg, B., Hervé, C., 2017. A review about brown algal

cell walls and fucose-containing sulfated polysaccharides: Cell wall context, biomedical

properties and key research challenges. Carbohydr. Polym. 175, 395–408.

https://doi.org/10.1016/j.carbpol.2017.07.082

Deniaud-Bouët, E., Kervarec, N., Michel, G., Tonon, T., Kloareg, B., Hervé, C., 2014. Chemical and

enzymatic fractionation of cell walls from Fucales: insights into the structure of the

extracellular matrix of brown algae. Ann. Bot. 114, 1203–1216.

https://doi.org/10.1093/aob/mcu096

Descamps, V., Colin, S., Lahaye, M., Jam, M., Richard, C., Potin, P., Barbeyron, T., Yvin, J.-C., Kloareg,

B., 2006. Isolation and Culture of a Marine Bacterium Degrading the Sulfated Fucans from

Marine Brown Algae. Mar. Biotechnol. 8, 27–39. https://doi.org/10.1007/s10126-005-5107-0

Domon, B., Costello, C.E., 1988. A systematic nomenclature for carbohydrate fragmentations in FAB-

MS/MS spectra of glycoconjugates. Glycoconj. J. 5, 397–409.

https://doi.org/10.1007/BF01049915

Ficko-Blean, E., Duffieux, D., Rebuffet, E., Larocque, R., Groisillier, A., Michel, G., Czjzek, M., 2015. Biochemical and structural investigation of two paralogous glycoside hydrolases from Zobellia galactanivorans: novel insights into the evolution, dimerization plasticity and catalytic mechanism of the GH117 family. Acta Crystallogr. Sect. -Struct. Biol. 71, 209–223. https://doi.org/10.1107/S1399004714025024

Giles, K., Ujma, J., Wildgoose, J., Pringle, S., Richardson, K., Langridge, D., Green, M., 2019. A Cyclic Ion Mobility-Mass Spectrometry System. Anal. Chem. 91, 8564–8573. https://doi.org/10.1021/acs.analchem.9b01838

Groisillier, A., Herve, C., Jeudy, A., Rebuffet, E., Pluchon, P.F., Chevolot, Y., Flament, D., Geslin, C., Morgado, I.M., Power, D., Branno, M., Moreau, H., Michel, G., Boyen, C., Czjzek, M., 2010. MARINE-EXPRESS: taking advantage of high throughput cloning and expression strategies for the post-genomic analysis of marine organisms. Microb. Cell Factories 9, 45. https://doi.org/10.1186/1475-2859-9-45

Guerra Dore, C.M.P., Faustino Alves, M.G. das C., Pofirio Will, L.S.E., Costa, T.G., Sabry, D.A., de Souza Rego, L.A.R., Accardo, C.M., Rocha, H.A.O., Filgueira, L.G.A., Leite, E.L., 2013. A sulfated polysaccharide, fucans, isolated from brown algae Sargassum vulgare with anticoagulant, antithrombotic, antioxidant and anti-inflammatory effects. Carbohydr. Polym. 91, 467–475. https://doi.org/10.1016/j.carbpol.2012.07.075

KLOAREG, B., B, K., M, D., M, Q., 1979. EXTRACTION ET PURIFICATION DU FUCOIDANE DE PELVETIA CANALICULATA (DENE ET THUR.). Extr. Purif. FUCOIDANE PELVETIA CANALICULATA DENE THUR.

Li, P., Jackson, G.P., 2017. Charge Transfer Dissociation (CTD) Mass Spectrometry of Peptide Cations: Study of Charge State Effects and Side-Chain Losses. J. Am. Soc. Mass Spectrom. 28, 1271–1281. https://doi.org/10.1007/s13361-016-1574-y

Lombard, V., Ramulu, H.G., Drula, E., Coutinho, P.M., Henrissat, B., 2014. The carbohydrate-active enzymes database (CAZy) in 2013. Nucleic Acids Res. 42, D490–D495. https://doi.org/10.1093/nar/gkt1178

Mabeau, S., Kloareg, B., Joseleau, J.-P., 1990. Fractionation and analysis of fucans from brown algae. Phytochemistry 29, 2441–2445. https://doi.org/10.1016/0031-9422(90)85163-A

Nagaoka, M., Shibata, H., Kimura-Takagi, I., Hashimoto, S., Kimura, K., Makino, T., Aiyama, R., Ueyama, S., Yokokura, T., 1999. Structural study of fucoidan from Cladosiphon okamuranus TOKIDA. Glycoconj. J. 16, 19–26. https://doi.org/10.1023/A:1006945618657

Niedermeyer, T.H.J., Strohalm, M., 2012. mMass as a Software Tool for the Annotation of Cyclic Peptide Tandem Mass Spectra. Plos One 7, e44913. https://doi.org/10.1371/journal.pone.0044913

Nishino, T., Nagumo, T., Kiyohara, H., Yamada, H., 1991. Studies on Polysaccharides from Ecklonia-Kurome .2. Structural Characterization of a New Anticoagulant Fucan Sulfate from the Brown Seaweed Ecklonia-Kurome. Carbohydr. Res. 211, 77–90. https://doi.org/10.1016/0008-6215(91)84147-7

Pluskal, T., Castillo, S., Villar-Briones, A., Orešič, M., 2010. MZmine 2: Modular framework for processing, visualizing, and analyzing mass spectrometry-based molecular profile data. BMC Bioinformatics 11, 395. https://doi.org/10.1186/1471-2105-11-395

Ponce, N.M.A., Stortz, C.A., 2020. A Comprehensive and Comparative Analysis of the Fucoidan Compositional Data Across the Phaeophyceae. Front. Plant Sci. 11, 556312. https://doi.org/10.3389/fpls.2020.556312

Ropartz, D., Giuliani, A., Fanuel, M., Herve, C., Czjzek, M., Rogniaux, H., 2016a. Online coupling of high-resolution chromatography with extreme UV photon activation tandem mass spectrometry: Application to the structural investigation of complex glycans by dissociative photoionization. Anal. Chim. Acta 933, 1–9. https://doi.org/10.1016/j.aca.2016.05.036

Ropartz, D., Li, P., Fanuel, M., Giuliani, A., Rogniaux, H., Jackson, G.P., 2016b. Charge Transfer

Dissociation of Complex Oligosaccharides: Comparison with Collision-Induced Dissociation

and Extreme Ultraviolet Dissociative Photoionization. J. Am. Soc. Mass Spectrom. 27, 1614–

1619. https://doi.org/10.1007/s13361-016-1453-6

Ropartz, D., Li, P., Jackson, G.P., Rogniaux, H., 2017. Negative Polarity Helium Charge Transfer

Dissociation Tandem Mass Spectrometry: Radical-Initiated Fragmentation of Complex

Polysulfated Anions. Anal. Chem. 89, 3824–3828.

https://doi.org/10.1021/acs.analchem.7b00473

Sakai, T., Ishizuka, K., Shimanaka, K., Ikai, K., Kato, I., 2003. Structures of oligosaccharides derived

from Cladosiphon okamuranus fucoidan by digestion with marine bacterial enzymes. Mar.

Biotechnol. 5, 536–544. https://doi.org/10.1007/s10126-002-0107-9

Salmeán, A.A., Guillouzo, A., Duffieux, D., Jam, M., Matard-Mann, M., Larocque, R., Pedersen, H.L.,

Michel, G., Czjzek, M., Willats, W.G.T., Hervé, C., 2018. Double blind microarray-based

polysaccharide profiling enables parallel identification of uncharacterized polysaccharides

and carbohydrate-binding proteins with unknown specificities. Sci. Rep. 8.

https://doi.org/10.1038/s41598-018-20605-9

Studier, F.W., 2005. Protein production by auto-induction in high-density shaking cultures. Protein

Expr. Purif. 41, 207–234. https://doi.org/10.1016/j.pep.2005.01.016

Vickers, C., Liu, F., Abe, K., Salama-Alber, O., Jenkins, M., Springate, C.M.K., Burke, J.E., Withers, S.G.,

Boraston, A.B., 2018. Endo-fucoidan hydrolases from glycoside hydrolase family 107 (GH107)

display structural and mechanistic similarities to -l-fucosidases from GH29. J. Biol. Chem. 293,

18296–18308. https://doi.org/10.1074/jbc.RA118.005134

Wang, Y., Xing, M., Cao, Q., Ji, A., Liang, H., Song, S., 2019. Biological Activities of Fucoidan and the

Factors Mediating Its Therapeutic Effects: A Review of Recent Studies. Mar. Drugs 17, 183.

https://doi.org/10.3390/md17030183

Yuguchi, Y., Tran, V.T.T., Bui, L.M., Takebe, S., Suzuki, S., Nakajima, N., Kitamura, S., Thanh, T.T.T.,

2016. Primary structure, conformation in aqueous solution, and intestinal

immunomodulating activity of fucoidan from two brown seaweed species Sargassum

crassifolium and Padina australis. Carbohydr. Polym. 147, 69–78.

https://doi.org/10.1016/j.carbpol.2016.03.101

Zablackis, E., Perez, J., 1990. A Partially Pyruvated Carrageenan from Hawaiian Grateloupia-Filicina

(cryptonemiales, Rhodophyta). Bot. Mar. 33, 273–276.

https://doi.org/10.1515/botm.1990.33.3.273

10. Legends to figures

Figure 1. Typical building blocks found in FCSPs from Fucales (including *P. canaliculata*), bearing one, two or three sulfate groups. The disaccharide repeating unit is: (a) A-type motif: [→4)α-L-fucopyranose-2-sulfate-(1→3)-α-L-fucopyranose-(1→] (2.Fuc + 1.S, DS/DP = 0.5). (b) B-type motif: [→4)α-L-fucopyranose-2-sulfate-(1→3)-α-L-fucopyranose-2-sulfate-(1→] (2.Fuc + 2.S, DS/DP = 1). (c) C-type motif: [4→)α-L-fucopyranose-2,3-disulfate-(1→3)-α-L-fucopyranose-2-sulfate-(1→] (2.Fuc + 3.S, DS/DP = 1.5). Fuc: fucose. DS: degree of sulfation. DP: degree of polymerization.

Figure 2. Oligofucans released by *Mf*FcnA represented by their DS/DP as a function of their DP, for different time points. (a) T=1H; (b) T=16H; (c) T=5 Days. The surface area of the sphere is proportional to the species intensity in MS. Species plotted in red only contain fucosyl residues and sulfates. Most intense species: (a) DP=10; DS/DP=1.5; I = 1.67e6; (b) DP=4; DS/DP=1.5; I = 1.37e6; (c) DP=4; DS/DP=1.5; I = 8.75e6. DS: degree of sulfation. DP: degree of polymerization.

Figure 3. Oligofucans released by *Mf*FcnA represented by their DS/DP as a function of their DP, for different time points. (a) T=1H; (b) T=16H; (c) T=5 Days. The surface area of the sphere is proportional to the species intensity in MS. Species plotted in blue: oligofucans containing fucose, sulfate(s) and one hexose. Species plotted in green: oligofucans containing fucose, sulfate(s) and one pentose. Most intense species: (a) DP=12; DS/DP=1.17; I = 2.14e5; (b) DP=10; DS/DP=1.2; I = 3.45e5; (c) DP=10; DS/DP=1.2; I = 4.89e5. DS: degree of sulfation. DP: degree of polymerization.

Figure 4. Annotated structures of two oligofucans released by *Mf*FcnA, which masses fitted with an ideal combination of pure C-type moieties. The fragments are those observed in the He-CTD fragmentation spectrum that led to an unambiguous positioning of the sulfates along the backbone for both structures. (a) DP4: (α-L-fucopyranosyl-2,3-disulfate-(1→3)-α-L-fucopyranosyl-2-sulfate)$_2$; (b) DP6: (α-L-fucopyranosyl-2,3-disulfate-(1→3)-α-L-fucopyranosyl-2-sulfate)$_3$

Figure 5. He-CTD mass spectrum of the ^{18}O-labelled FCOS of DP6 with one hexose (5.Fuc + 1.Hex + 8.S) isolated for fragmentation as [M-8.H+10.HxA]$^{2+}$ at *m/z* 1282.6. Lower panel (left): annotated structure; the fragments displayed are those that led to this structural proposition, as discussed in the text.

Figure 6. He-CTD mass spectrum of the ^{18}O-labelled DP9 oligofucan with one pentose (8.Fuc + 1. Pen + 8.S) isolated for fragmentation as [M-8.H+10.HxA]$^{2+}$ at *m/z* 1486.8. Lower panel (left): annotated structure; the fragments displayed are those which led to this structural proposition, as discussed in the text.

Figure 7. Schematic representation of the subsite-binding specificity in the catalytic cleft of *Mf*FcnA. The relative position of substrate sugar-units is provided with respect to the eight predicted subsites within the enzyme's active site (numbered from -4 to +4). The point of cleavage is indicated by a grey triangle. Subsites -2/-1 and +1/+2 can only accommodate a C moiety. Subsites -4/-3 can accommodate moieties B or C. Subsites -4/-3 can accommodate B or C moieties or can be unoccupied.
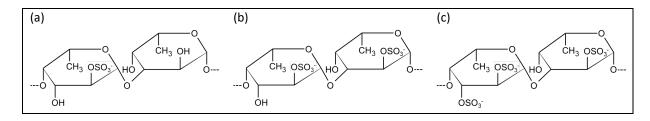
11. Figures

Figure 1.

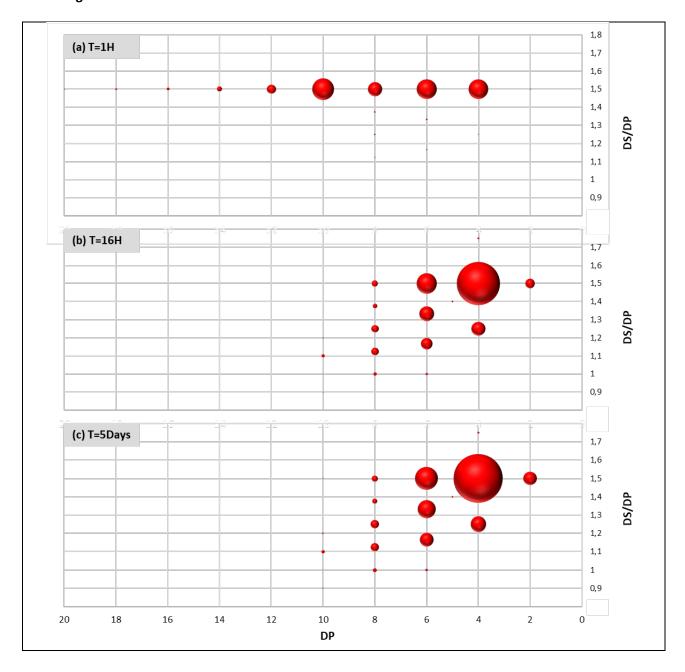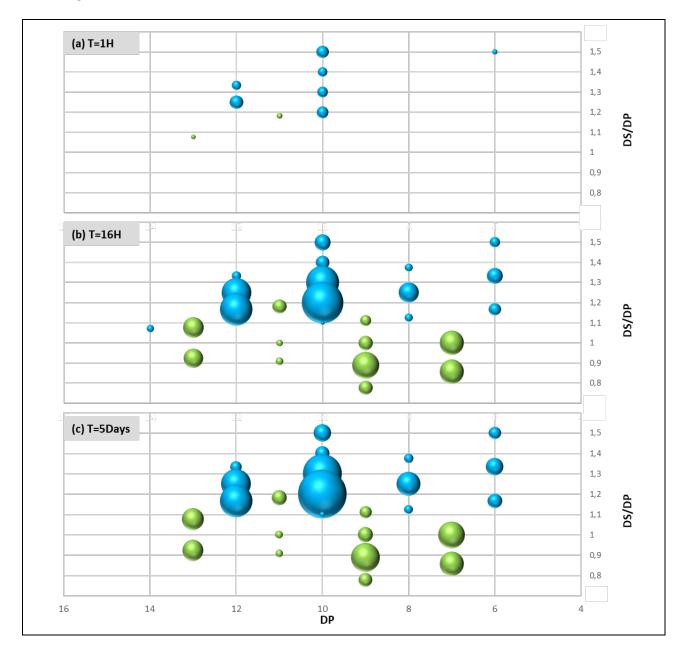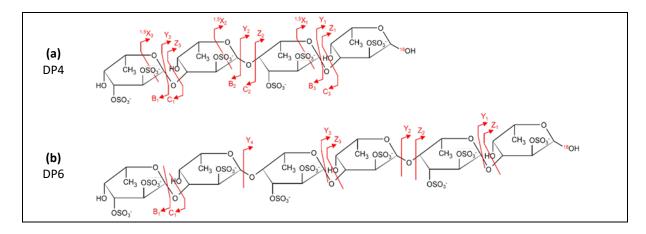

Figure 2.

Figure 3.

Figure 4.

(a)
DP4

(b)
DP6

Figure 5.

Legend :
- Loss of [HxA+SO₃] (181.07 Da)
- Loss of [HxA] (101.12 Da)
- Loss of Hexose (162.05 Da)
- Loss of H₂O (18.01 Da)

Figure 6.

Figure 7.